Electronic Supplementary Material (ESI) for Nanoscale.

Supporting Information

The Enhanced Raman Scattering on Two-Dimensional Palladium Diselenide

Zehong Lei, Xinkuo Zhang, Yu Zhao, Aixiang Wei, Lili Tao,* Yibin Yang, Zhaoqiang Zheng, Li Tao, Peng Yu, and Jingbo Li*

zhaoyu@gdut.edu.cn & taoll@gdut.edu.cn

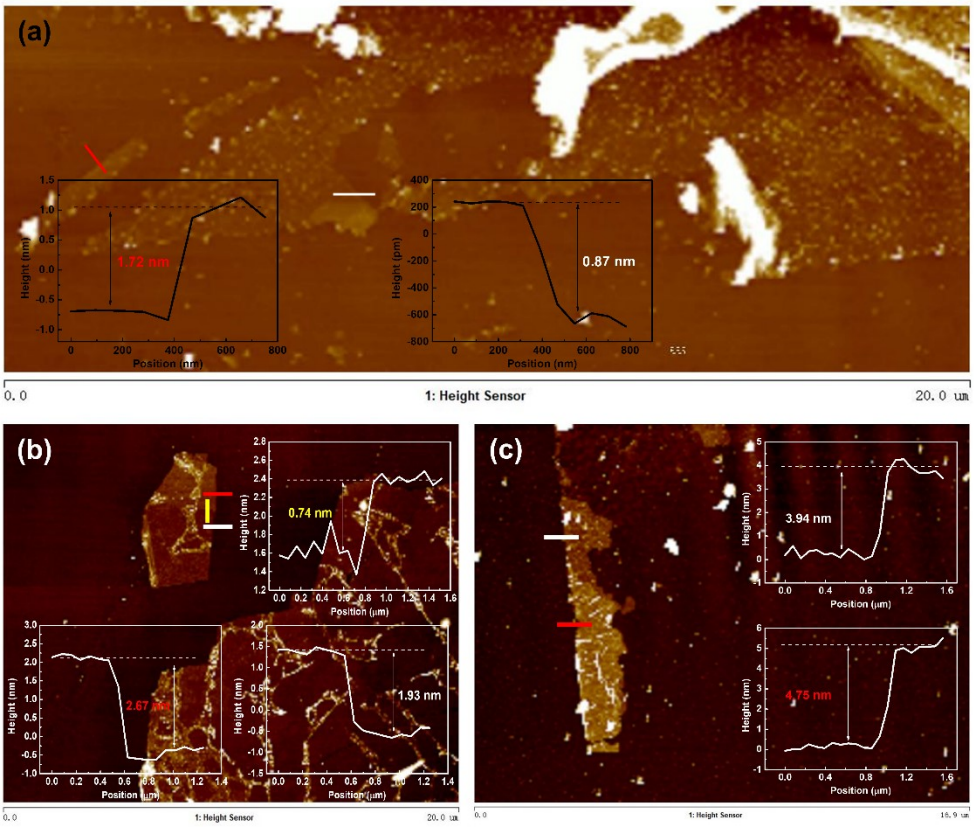

Figure S1. The AFM image of $PdSe_2$ with different layer numbers on mica. Each thickness for different positions was marked with relative color.

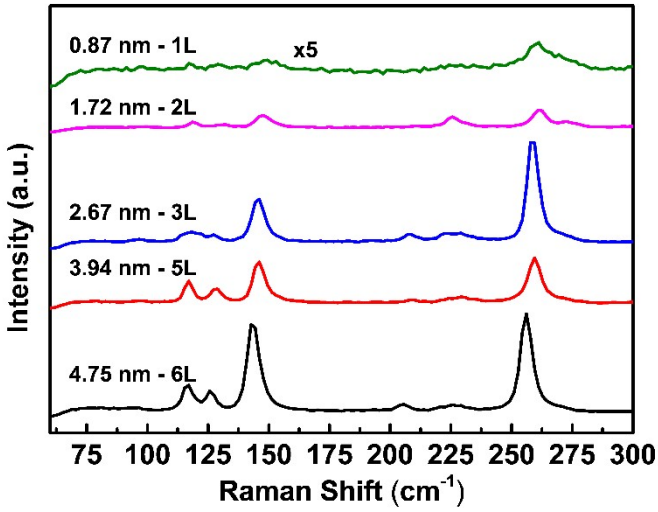

Figure S2. The Raman spectra of $PdSe_2$ with different layer numbers. The measured $PdSe_2$ samples are the same ones in **Figure S**1 after transferred to SiO_2/Si substrate.

Table S1. The average intensity of Si peak with the corresponding layers. Each Si peak was randomly collected on the same flakes, using NOST FEX with the acquisition time of 5 s.

Spot	Bare SiO_2	1L	2L	3L	5L
1	4109	3102	2461	2133	1476
2	4078	3128	2460	2098	1630
3	4110	3180	2457	2158	1597
4	4227	3088	2471	2205	1628
5	4118	3124	2462	2195	1609
Average	4128	3124	2462	2158	1588
Normalization	1.32	1.00	0.79	0.69	0.51

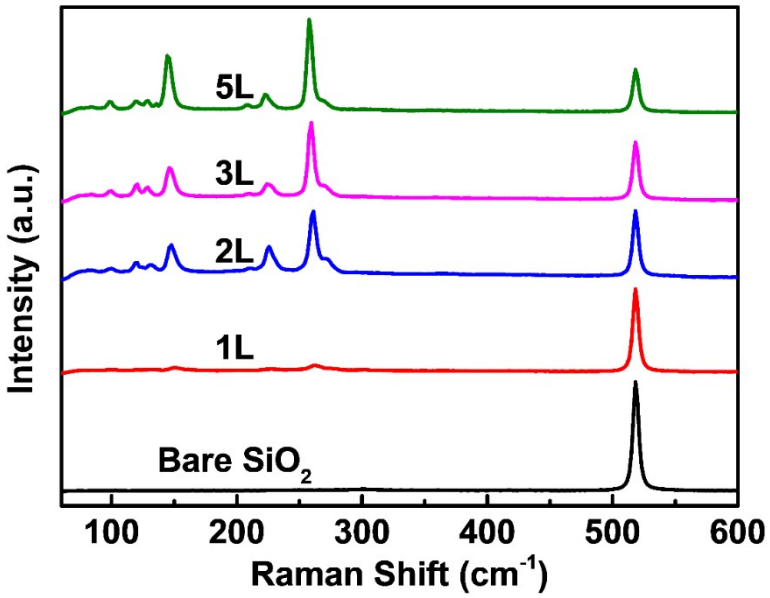

Figure S3. The Si signal intensity follows the changes of the layer numbers of $PdSe_2$.

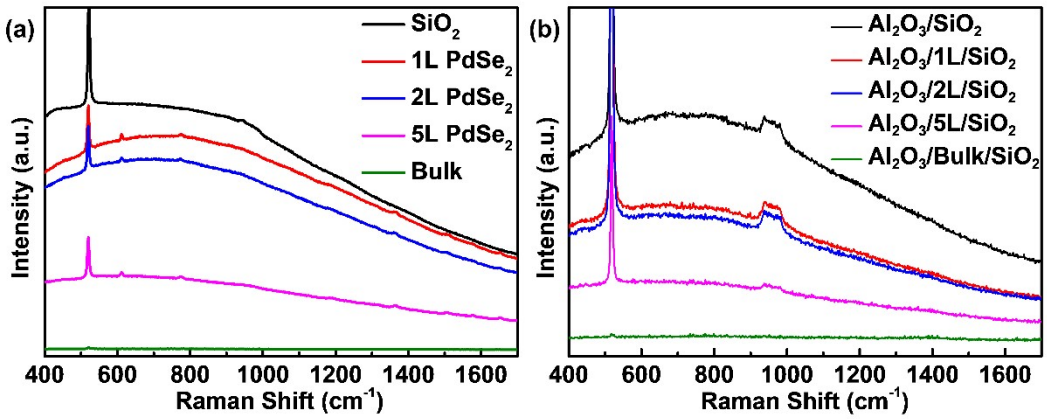

Figure S4. (a) Raman spectra for 10^{-6} M R6G coated on different substrates without baseline correction. (b) The relative Raman spectra of 10^{-6} M R6G on monolayer $PdSe_2$ with the deposition of Al_2O_3. Noted that the strong peak at about 1000 cm^{-1} is the second-order Raman scattering from the silicon substrate.

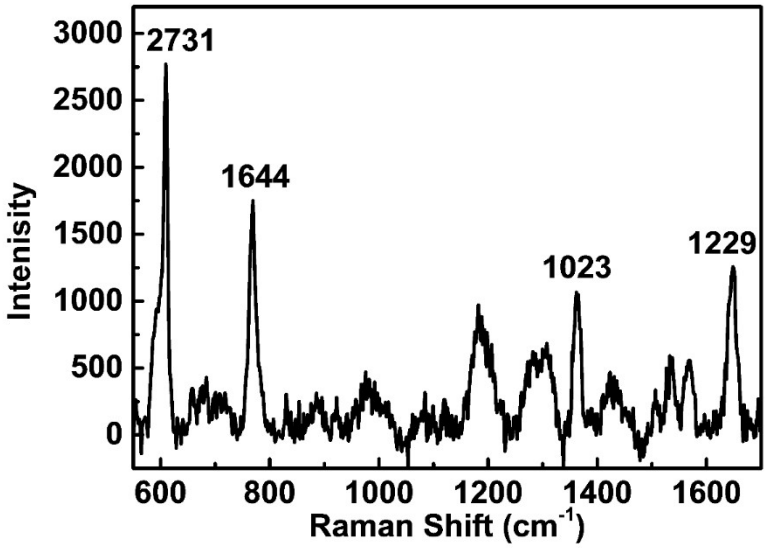

Figure S5. Raman spectra of bulk R6G prepared by the drying off of 5 μL 10^{-4} M water solution on a 285 nm SiO_2/Si substrate. Raman spectra was obtained using the LabRAM HR Evolution system with a laser power of 10 mW, acquisition time of 1 s and accumulation times of 3 times.

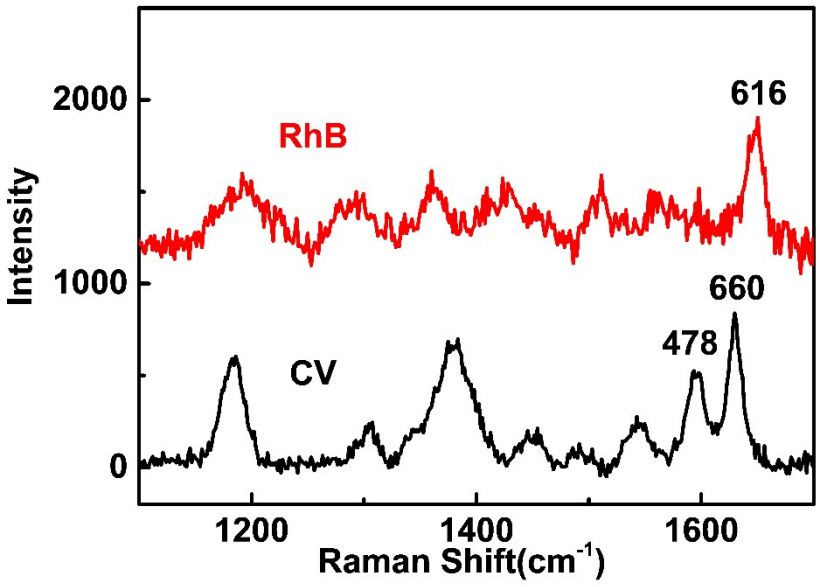

Figure S6. Raman spectra of bulk RhB and CV. RhB is obtained by the drying off of 5 μL 10^{-3} M water solution on a 285 nm SiO_2/Si substrate. Raman spectra was obtained using the LabRAM HR Evolution system with a laser power of 10 mW, acquisition

time of 1 s and accumulation times of 3 times. CV is obtained by the drying off of 5 μL 10^{-4} M water solution on a 285 nm SiO_2/Si substrate. Raman spectra was obtained using LabRAM HR Evolution system with a laser power of 10 mW, acquisition time of 5 s and accumulation times of 5 times...

In our work, we use analytes with a concentration of 10^{-4} M as the referenced bulk sample. The average thickness of the referenced analytes is lower than 100 nm, which is far smaller than the laser penetration depth of 21 and 40 μm for our Horiba LabRAM HR Evolution system and NOST FEX (South Korea), respectively. So, the Raman enhancement factors (EFs) can be valued by the following equation: [1]

$$EF = \frac{I_{SERS}}{I_{RS}} \times \frac{N_{RS}}{N_{SERS}} \quad (1)$$

$$N_{RS} = N_A n R_I^2 / R_{dif}^2 \quad (2)$$

$$N_{SERS} = N_A n \pi R_I^2 / S_{sub} \quad (3)$$

where I_{SERS} and I_{RS} are the SERS intensities and the intensity of bulk probe molecules in Raman spectra, respectively. And N_{SERS} and N_{RS} are the mounts of probed molecules in the SERS experiment and the amount of bulk probed molecules in the normal Raman experiment, respectively. The number of probe molecules can be estimated by formula (2) and (3), where N_A is the Avogadro's constant, n refers to the molar quantity of probe molecules, R_I refers to the radius of laser spot area (~ 1 μm), R_{dif} refers to the radius of the drop of the 5μL 10^{-4} M water solution on the silicon substrate (~ 0.1 cm), S_{sub} refers to the silicon substrate area (~ 2 cm^2). In this paper, R6G was used to estimate the Raman EF of $PdSe_2$.

For the EF of 10 μL 10^{-9} M R6G:

$$N_{RS} = 6.02\times10^{23}\times5\times10^{-6}\times10^{-4}\times\frac{1}{10^{6}} = 3.01\times10^{9}$$

$$N_{SERS} = 6.02\times10^{23}\times10^{-9}\times10\times10^{-6}\times\frac{3.14}{2\times10^{8}} = 94.51$$

$$EF = 0.1\times\frac{193}{2731}\times\frac{3.01\times10^{9}}{94.51}\approx 2.25\times10^{5}$$

Table S2. The SERS intensities of R6G in different concentrations and Raman Shift.

Wavenumber / Concentration	615 cm^{-1}	771 cm^{-1}	1351 cm^{-1}	1652 cm^{-1}
10^{-6} M	1915	667	325	266
10^{-7} M	553	192	164	123
10^{-8} M	315	132	101	76
10^{-9} M	193	56	58	39

Table S3. The EFs in different concentrations and Raman Shift for R6G.

Wavenumber / Concentration	615 cm^{-1}	771 cm^{-1}	1351 cm^{-1}	1652 cm^{-1}
10^{-6} M	2333.14	1292.09	1011.76	689.28
10^{-7} M	6448.99	3719.53	5105.71	3187.43
10^{-8} M	36738.68	2557.177	3144.37	1969.47
10^{-9} M	225073.48	108486.31	180568.12	101065.15

Table S4. The EFs for 10^{-6} M RhB.

Wavenumber	I_{RS}	I_{SERS}	EF

1650 cm^{-1}	616	70	90.2

Table S5. The EFs for 10^{-7} M CV.

Wavenumber	I_{RS}	I_{SERS}	EF
1581 cm^{-1}	475	65	139.5
1620 cm^{-1}	660	73	112.7

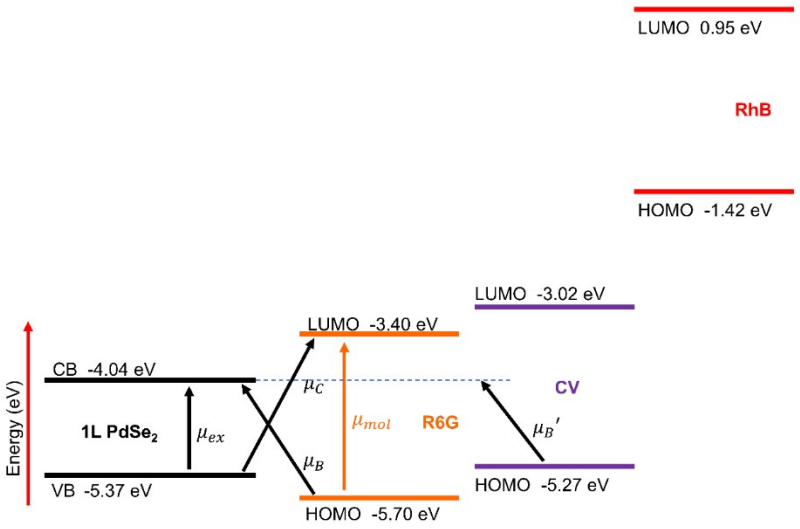

Figure S7. The schematic diagram of the relative position of the energy bands between molecules and monolayer $PdSe_2$.

We speculated that the different detection limits and EF of the three molecules can be attributed to the difference in the photoinduced charge transfer (PICT) processes. We investigate the band alignment between the molecules and monolayer $PdSe_2$ (see **Figure S**7) to discuss the possible mechanism behind. The energy bands of RhB are far away from the conduction band minimum (CBM) of the monolayer $PdSe_2$, possibly resulting in the weakest PICT process among the three molecules. The electrons can be excited from the HOMO of R6G and CV to the CBM of $PdSe_2$ (transition of μ_B and μ_B' in the figure) since the excitation energy is larger than the energy difference between HOMO of molecules and CBM of monolayer $PdSe_2$. However, the hole transferred from the valence band maximum (VBM) to the LUMO of CV is not allowed as the excitation energy needed (2.35 eV) is slightly larger than the energy of laser, while the same process for R6G (transition of μ_c) is possible due to its lower LUMO position.

Thereby, the PICT is more efficient for R6G than CV when coupled with monolayer $PdSe_2$. The discussion of the charge transfer process using the band structure of the molecules and 2D $PdSe_2$ well explained the different detection limits and EF for the three molecules.

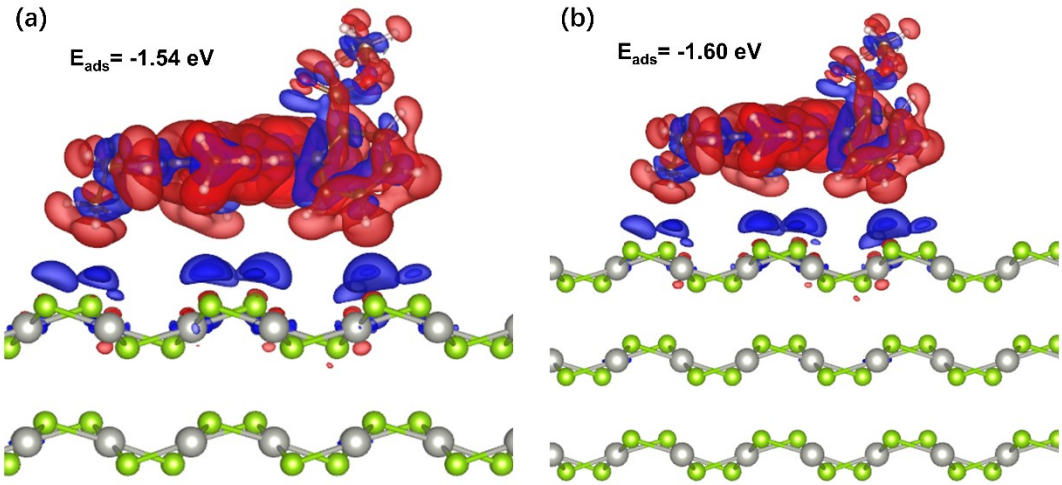

Figure S8. Charge density difference of R6G adsorption on bilayer (a) and trilayer (b) $PdSe_2$.

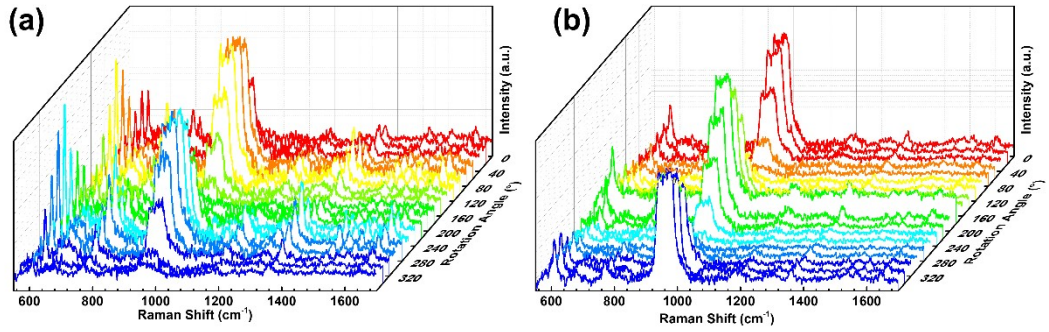

Figure S9. Anisotropic Raman enhancement measurement. Angle-resolved polarized Raman spectra of R6G (10^{-6} M) under the (a) parallel and (b) cross configurations. Noted that the strong peak at about 1000 cm^{-1} is the second-order Raman scattering from the silicon substrate.

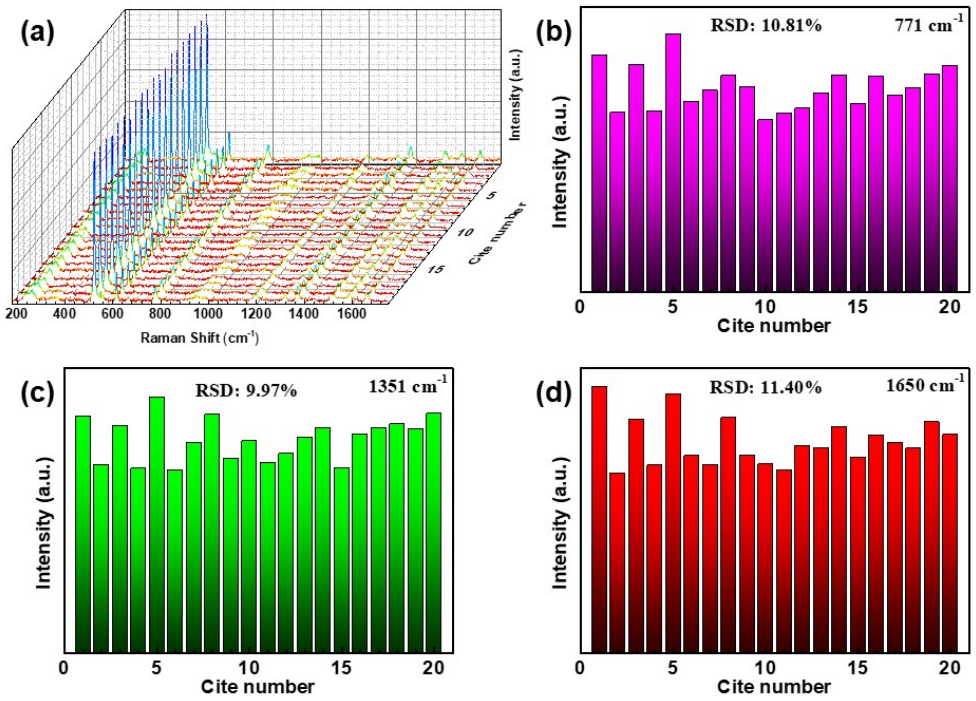

Figure S10**.** Uniformity of SERS signal on $PdSe_2$ substrate. (a) SERS spectra of R6G (10^{-6} M) collected from 20 randomly selected sites on monolayer $PdSe_2$. (b-d) Histogram distribution of the Raman intensities at (b)771 cm^{-1}, (c)1351 cm^{-1}, and (d)1650 cm^{-1}.

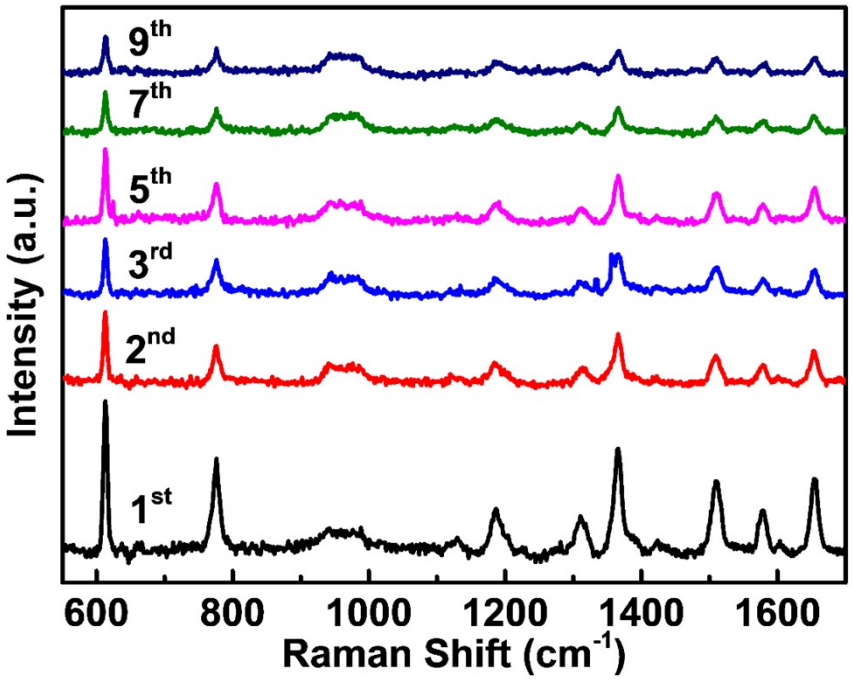

Figure S11**.** Raman spectra of R6G (10^{-6} M) on monolayer $PdSe_2$ at the same spot for increased measured times.

Raman spectra of the R6G molecule at the same spot for different collecting times were demonstrated in **Figure S**11. Each collection was exposed to 532 nm laser for 25 seconds (acquisition for five seconds and accumulation for five times). An obvious reduction of R6G signal intensity was found via a comparison between the first collection and the second collection. After eight collections, only 14.5 % Raman signal intensity remained in the ninth collection at 615cm^{-1}. The photobleaching is usually observed on conventional SPR-based SERS substrates rather than on 2D materials.[2] It is commonly believed that 2D materials have a negligible photobleaching effect as the excitation state of molecules excited by laser can rapidly relax to the ground state through the additional path provided by a charge transfer of substrate. The obvious photobleaching effect may probably originate from the indirect band structure of 2D

$PdSe_2$. The indirect bandgap of few-layer $PdSe_2$ may prolong the lifetime of the excited electrons,[3, 4] leading to the lower chemical potential difference between R6G and $PdSe_2$ and a consequential suppression of the charge transition from LUMO of the molecule to CB of the substrate. We suggest a suitable power of the excitation laser should be adopted to balance the requirement of an excellent signal of SERS and the reduction of the photobleaching effect.

Table S6. Comparison of the SERS performances among various 2D materials. h-BN: hexagonal boron nitride. CuPc: copper phthalocyanine. MB: methylene blue. CV: crystal violet.

Stability: Stability of SERS. The approximate ratio of Raman signal intensity after to before exposed in the air for a certain period.

SERS material	Analyte -Excitation wavelength (nm)	LOD（M）	EF	Stability	Reference
$PdSe_2$	R6G – 532 nm	10^{-9}	2.2×10^{5}	1(30day)	This work
Graphene	R6G – 514 nm	8×10^{-9}	N/A	N/A	5
h-BN	CuPc – 633 nm	Lower than MoS_2	N/A	N/A	6
2H-MoS_2	R6G – 532 nm	5×10^{-6}	N/A	N/A	7
1T-MoS_2	R6G – 532 nm	10^{-9}	2.92×10^{4}	N/A	8
1T-$MoSe_2$	R6G – 532 nm	10^{-8}	N/A	N/A	9
1T'-ReS_2	R6G – 532 nm	10^{-9}	N/A	N/A	10

SERS material	Analyte -Excitation wavelength (nm)	LOD（M）	EF	Stability	Reference
1T'-WTe_2	R6G – 532 nm	4×10^{-14}	1.8×10^{9}	0.75(12day)	2
1T'-$MoTe_2$	R6G – 532 nm	4×10^{-13}	1.6×10^{8}	N/A	2
NbS_2	MB – 633 nm	10^{-14}	N/A	0.25(30day)	11
$NbSe_2$	R6G – 532 nm	5×10^{-16}	N/A	0.25(35day)	12
$NbTe_2$	R6G – 532 nm	10^{-9}	1.37×10^{6}	N/A	13
$PtSe_2$	R6G – 532 nm	10^{-9}	1.3×10^{5}	N/A	14
GaN	CV – 532 nm	2×10^{-7}	5.2×10^{5}	0.9(60day)	15

References

1. A. I. Pérez-Jiménez, D. Lyu, Z. Lu, G. Liu, B. Ren, *Chem. Sci.*, 2020, **11**, 4563-4577.
2. L. Tao, K. Chen, Z. Chen, C. Cong, C. Qiu, J. Chen, X. Wang, H. Chen, T. Yu, W. Xie, S. Deng, J. B. Xu, *J. Am. Chem. Soc.*, 2018, **140**(28), 8696-8704.
3. A. D. Oyedele, S. Yang, L. Liang, A. A. Puretzky, K. Wang, J. Zhang, P. Yu, P. R. Pudasaini, A. W. Ghosh, Z. Liu, C. M. Rouleau, B. G. Sumpter, M. F. Chisholm, W. Zhou, P. D. Rack, D. B. Geohegan, K. Xiao, *J. Am. Chem. Soc.*, 2017, **139**, 14090−14097.
4. H. Kim, H. J. Choi, *Phys. Rev. B*, 2021, **103**, 165419.
5. X. Ling, L. Xie, Y. Fang, H. Xu, H. Zhang, J. Kong, M. Dresselhaus, J. Zhang, Z. Liu, *Nano Lett.*, 2010, **10**(2), 553-561.
6. X. Ling, W. Fang, Y. Lee, P. Araujo, X. Zhang, J. Rodriguez-Nieva, Y. Lin, J. Zhang, J. Kong, M. Dresselhaus, *Nano Lett.*, 2014, **14**(6), 3033−3040.

7. Y. Lee, H. Kim, J. Lee, S. H. Yu, E. Hwang, C. Lee, J. H. Ahn, J. H. Cho, *Chem. Mater.*, 2016, **28**(1), 180-187.
8. E. Er, H. L. Hou, A. Criado, J. Langer, M. Möller, N. Erk, L. M. Liz-Marzán, M. Prato, *Chem. Mater.*, 2019, **31**(15), 5725-5734.
9. Y. Yin, P. Miao, Y. Zhang, J. Han, X. Zhang, Y. Gong, L. Gu, C. Xu, T. Yao, P. Xu, Y. Wang, B. Song, S. Jin, *Adv. Funct.Mater.*, 2017, **27**(16), 1606694.
10. P. Miao, J. K. Qin, Y. Shen, H. Su, J. Dai, B. Song, Y. Du, M. Sun, W. Zhang, H. L. Wang, C. Y. Xu, P. Xu, *Small*, 2018, **14**, 1704079.
11. X. Song, Y. Wang, F. Zhao, Q. Li, H. Q. Ta, M. H. Rümmeli, C. G. Tully, Z. Li, W. J. Yin, L. Yang, K. B. Lee, J. Yang, I. Bozkurt, S. Liu, W. Zhang, M. Chhowalla, *ACS Nano*, 2019, **13**, 8312-8319.
12. Q. Lv, X. Wu, J. Tan, B. Liu, L. Gan, J. Li, Z. H. Huang, F. Kang, R. Lv, *J. Mater. Chem. A*, 2021, **9**, 2725-27331.
13. K. Wang, Z. Guo, Y. Li, Y. Guo, H. Liu, W. Zhang, Z. Zou, Y. Zhang, Z. Liu, *ACS Appl. Nano Mater.*, 2020, **3**(11), 11363-11371.
14. X. Hou, X. Tang, Y. Wei, S. Wang, Q. Hao, J. M. Hou, T. Qiu, *Cell Reports Physical Science*, 2021, **2**(7), 100488.
15. S. Zhao, H. Wang, L. Niu, W. Xiong, Y. Chen, M. Zeng, S. Yuan, L. Fu, *Small*, 2021, **17**, 2103442.